

1 **Nonlinear reconstruction of bioclimatic outdoor-environment**
2 **dynamics for the Lower Silesia region (SW Poland)**

3 **Arkadiusz Głogowski¹ · Paolo Perona^{2,3} ·**
4 **Krystyna Bryś¹ · Tadeusz Bryś⁴**

5
6 Received: date / Accepted: date

7 **Abstract** Measured meteorological time series are frequently used to obtain information
8 about climate dynamics. We use time series analysis and nonlinear system identification
9 methods in order to assess outdoor-environment bioclimatic conditions starting from the
10 analysis of long historical meteorological data records. We investigate and model the stochas-
11 tic and deterministic properties of 117 years (1891-2007) of monthly measurements of air
12 temperature, precipitation and sunshine duration by separating their slow and fast compo-
13 nents of the dynamics. In particular, we reconstruct the trend behaviour at long terms by
14 modelling its dynamics via a phase space dynamical systems approach. The long-term re-
15 construction method reveals that an underlying dynamical system would drive the trend
16 behaviour of the meteorological variables and in turn of the calculated Universal Thermal
17 Climatic Index (UTCI), as representative of bioclimatic conditions. At longer terms, the
18 system would slowly be attracted to a limit cycle characterized by 50-60 years cycle fluctu-
19 ations that is reminiscent of the Atlantic Multidecadal Oscillation (AMO). Because of lack
20 of information about long historical wind speed data we performed a sensitivity analysis of
21 the UTCI to three constant wind speed scenarios (i.e., 0.5, 1 and 5 m/s). This methodology

A. Głogowski
E-mail: arkadiusz.glogowski@upwr.edu.pl ·
T. Bryś
E-mail: tbrys@tlen.pl ·
K. Bryś
E-mail: krystyna.brys@upwr.edu.pl ·
P. Perona
E-mail: paolo.perona@epfl.ch

¹Institute of Environmental Protection and Development, Faculty of Environmental Engineering and Geodesy, Wrocław University of Environmental and Life Science, pl. Grunwaldzki 24; 50-363 Wrocław – Poland

²School of Engineering, The University of Edinburgh, Mayfield Road EH93JL, Edinburgh, United Kingdom

³Ecological Engineering Laboratory (ECOL), Institute of Environmental Sciences and Technology (IIE), ENAC Faculty, Ecole Polytechnique Federale del Lausanne (EPFL), Lausanne, Switzerland

⁴Polish Geophysical Society, Wrocław Division
pl. Grunwaldzki 24, 50-357 Wrocław, Poland

22 may be transferred to model bioclimatic conditions of nearby regions lacking of measured
23 data but experiencing similar climatic conditions.

24 **Keywords** UTCI · outdoor environment · time-series · machine learning · AMO

25 1 Introduction

26 The study of bioclimatic conditions of the outdoor environment is a very important sub-
27 ject, in the first instance to understand how climate changes may affect society's well being
28 (Stocker et al., 2013). Bioclimatic assessment has found applications in a multitude of re-
29 search areas relating the effects of climate change (Wu et al., 2019) on health and well-being
30 (Bröde et al., 2018), epidemiology (Di Napoli et al., 2018), military (Galan and Guedes,
31 2019), urban planning, etc. Di Napoli et al. (2018) correlated the Universal Thermal Climate
32 Index (henceforth referred to as UTCI) and mortality after intense heat waves in Europe.
33 Chinese tourism assessment was also explained by means of UTCI dynamics (Ge et al.,
34 2017). In Australia, Coutts et al. (2016) quantified the variability of outdoor environment
35 near central business centres in Melbourne. Ndetto and Matzarakis (2015) also used UTCI
36 to asses bioclimatic conditions of the urban environment in Tanzania. Eventually, Bröde
37 et al. (2012) studied outdoor thermal comfort in Brazil. These studies find practical applica-
38 tion for instance to determine the attractiveness of tourist places like coastal and mountain
39 towns or health resorts in such areas (Ge et al., 2017; Błażejczyk and Kunert, 2011), as well
40 as in ergonomics to determine working conditions in both indoor and outdoor environments
41 (Bröde et al., 2018; Sen and Nag, 2019).

42 Over 200 bioclimatic indexes were proposed in the last 100 years and used to analyze hu-
43 man body's response to outdoor environmental conditions (de Freitas and Grigorieva, 2017).
44 Early methods to assess bioclimate conditions involved simple indexes based on a single pa-
45 rameter, e.g. like physical saturation deficit (Thilenius and Dorno, 1925), or Wet Bulb Tem-
46 perature T_{wb} (Haldane, 1905). Notice how such variables describe meteorological processes
47 rather than bioclimatic conditions. More advanced bioclimatic indexes use human biological
48 variables (e.g., body temperature or energy (heat) exchange) in relation to actual meteorolo-
49 gical conditions in order to derive the Physiological Equivalent Temperature, PET, (Mayer
50 and Höppe, 1987), or the UTCI (Błażejczyk et al., 2013; Jendritzky et al., 2012). Many bio-
51 climatic indexes are commonly build up using heat exchange (led by sunshine duration), air
52 temperature or air humidity (led by precipitation) in parallel with atmospheric pressure and
53 wind speed (Fiala et al., 2012; Masterson and Richardson, 1979; Bosford, 1971). In April of
54 2009 The World Meteorological Organization (WMO) officially promoted the use of UTCI
55 as the most suitable tool for determining bioclimatic conditions at the international sym-
56 posium (WMO, 2009). Additionally, in last decade many Polish scientists have used UTCI
57 in different parts of Poland and they confirmed that this index is well suited for describing
58 conditions of polish climate (Błażejczyk et al., 2010, 2012, 2013; Chabior, 2011; Kuch-
59 cik et al., 2013; Okoniewska and Więclaw, 2013; Nidzgorska-Lencewicz, 2015; Bryś and
60 Ojrzyńska, 2016; Rozbicka and Rozbicki, 2016, 2018). It is worth noticing that quantities
61 like sunshine duration, air temperature and precipitation are among the basic meteorolog-
62 ical variables used to characterize local and global both weather and climate conditions
63 (Brönnimann, 2015). Solar energy reaching Earth's upper atmosphere is the direct engine of
64 the Earth's climate and its dynamics (Kondratyev, 2013). Air circulation affects the spatial
65 and temporal distribution of the above mentioned meteorological quantities and thus it con-
66 tributes to sustain Earth's climate system. Globally, climate conditions depend on mass and

67 energy fluxes, which affect both nature biodiversity at meso and global scales, and outdoor
68 bioclimatic conditions for human body at the local scale (Bryś et al., 2020).

69 Air temperature is widely recognised to be a fundamental proxy variable for the as-
70 sessment of climate conditions and related changes (Stocker et al., 2013). It is linked to
71 sunshine (e.g., number of sunny days) and to air mass conditions (i.e. humidity), and so
72 indirectly to rainfalls and evaporation processes. There is also increasing evidence about the
73 forcing role played by intensive human activity, whose effects are considered to be respon-
74 sible for accelerating the rate of climatic changes (Stocker et al., 2013; Brönnimann, 2015).
75 Studying long-term air temperature evolution in relation to sunshine duration and precipita-
76 tion is thus meaningful from a climatological viewpoint (Flohn, 1957; Girs, 1971; Bryson,
77 1974; Groveman and Landsberg, 1979). For example, Wrocław’s climate at specific loca-
78 tions results from the interaction between oceanic and continental air masses. Measurements
79 at these locations provide an opportunity to better assess bioclimatic variability from obser-
80 vations (Kosiba, 1948; Dubicka, 1994). At sufficient large time scales, one would expect the
81 link between sunshine duration, precipitation and air temperature to emerge as a slow com-
82 ponent of the climate dynamics to which high frequency (correlated) stochastic fluctuations
83 are superimposed as fast components. Reconstructing both components dynamics is the first
84 step for advancing bioclimatological insights.

85 In this work we first extract the deterministic slow component linking precipitation, sun-
86 shine duration and temperature dynamics in a mechanistic way and then separate it from the
87 fast component that has a high dimensional origin (i.e., eventually stochastic). Notice, that
88 for these steps wind data records are only of minor importance as the above variables already
89 contain the effect of air circulation. In this sense, wind speed would be a redundant variable.
90 However, wind speed is of importance for the calculation of the UTCI where wind velocity
91 has a clear effect on body-felt bioclimatic conditions. Analysis of the slow component shows
92 that the dynamic is linked to Oceanic Oscillations such the North Atlantic Oscillation (NAO)
93 or Atlantic Multidecadal Oscillation (AMO) (Marsz et al., 2019; Niedźwiedz et al., 2009;
94 Malik et al., 2018; Knudsen et al., 2011). Malik et al. (2018) stress that oceanic oscillations
95 like AMO, Pacific decadal oscillation (PDO) or El-Niño southern oscillation (ENSO) are
96 mostly driven by sun activity and influence Sea Surface Temperature (SST) (Otterå et al.,
97 2010; Peng et al., 2013; Niedzielski, 2014, 2011). Using the UTCI as reference index, we
98 show that successful signal decomposition may not only provide insights about the dynam-
99 ics of the climate system at large time scale, but also offer a new methodology to calculate
100 bioclimatic indexes at long-terms.

101 **2 Materials and methods**

102 **2.1 Geographical location and data**

103 Wrocław (SW Poland) has one of the longest measured time series of air temperature and
104 precipitation in the World, its origins began in 1791. These series were reconstructed and
105 homogenized from data measured over 10 different locations in Wrocław. The basis of this
106 homogenization is from Wrocław university meteorological tower (known as Breslau Stern-
107 warte), where measurements were taken in the period 1791-1920. Successive almost 100
108 years were homogenized from other 9 stations due to the numerous administrative decisions
109 and technological improvements determining location changes. A comprehensive explana-
110 tion of this homogenization may be found in the works by Bryś and Bryś (2010a, 2005).
111 Here it suffices to say that homogenization and reconstructions techniques enabled to ob-

tain an information about other meteorological variables like sunshine duration and water vapour pressure. Closer details of how sunshine duration time series (since 1891) were obtained may also be found in Bryś and Bryś (2003), whereas about water vapour pressure (since 1883) we refer to the work of Bryś and Bryś (2001).

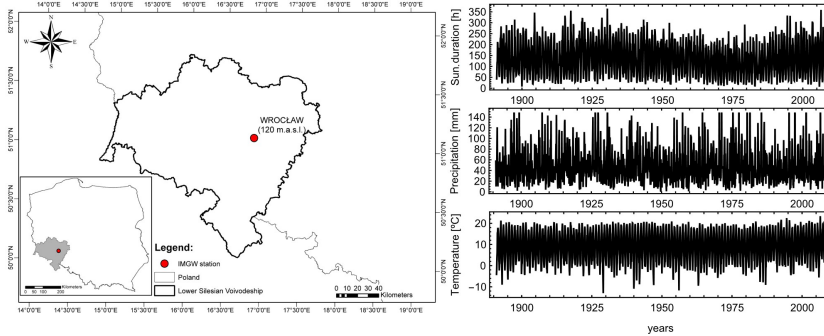


Fig. 1 Localization of analyzed area in Poland (left), with raw-data in years 1891-2007 (right)

Data used in the following work accounts for monthly sums of hours of sunshine duration (s) and precipitation (p), as well as monthly averages for air temperature (t) in Wrocław for period 1891-2007 (Fig. 1). The above said variables are typically used as a proxy for computing other quantities such, solar radiation (R), cloudiness (N), water vapour pressure (e), whence the importance of modelling them for forecasting purposes. As far as wind is concerned, this variable was extracted from the repository of the Polish Institute of Meteorology and Water Management National Research Institute (IMGW) using the “climate” package in R (Czernecki et al., 2020) and was only available for the 1966-2019. In general, monthly mean values for wind speed fluctuate between 0 and 4.9 m/s, being this the highest mean monthly wind speed observed in Wrocław (1966-2019). In Wrocław (1966-2019) mean monthly sum insolation oscillate between 40.7 h in December to 206 h in August with annual mean 1490.62 h. Mean monthly sum of precipitation change between 25.2 mm in February to 89.9 mm in July with annual sum 565.6 mm, Mean monthly temperature is equal -0.1 °C in January and reach 19.7 °C in July, the mean annual value of air temperature is equal 9.6 °C

2.2 Separation of the slow and fast signal components

All time series are clearly non-stationary because of the presence of a long-term trend affecting the data (Fig. 1). This phenomenon is typical of climatic data at all scales, and over the period of available measurements is considered an evidence of changes occurring in the Anthropocene (Brönnimann et al., 2019). Each data series was further decomposed by separating the slow component, $x_s(t)$ representing the non-linear, long-term trend from the fast component, $x_f(t)$, which represents the seasonal and the stochastic components affecting each meteorological variable (Brockwell and Davis, 2016)

$$x(t) = x_s(t) + x_f(t). \quad (1)$$

139 The long-term trend $x_s(t)$ was obtained by first performing a ten-years moving average
 140 with symmetric window, and then a frequency (i.e., Fourier) analysis of the resulting signals,
 141 which enhanced the dominant frequency still affecting all data series. The moving averaged
 142 data was then filtered at that identified frequency by using a low-pass Butterworth algorithm.
 143 This produced the data series $x_s(t)$ with which the original data were eventually detrended
 144 from the slow component.

145 The fast component, $x_f(t)$, thus resulted from removing the slow component from the
 146 original data. However, $x_f(t)$ still accounts for yearly seasonal (i.e. periodic) variability
 147 $x_{f_p}(t)$ affecting both the mean and the variance, and monthly correlated fluctuations $x_{f_c}(t)$,
 148 so that the original data was further decomposed as

$$x(t) = x_s(t) + x_f(t) = x_s(t) + x_{f_p}(t) + x_{f_c}(t), \quad (2)$$

149 as described in the next paragraph.

150 2.3 Modeling the fast component $x_f(t)$

151 Seasonal fluctuations $x_{f_s}(t)$ were very well described by the monthly mean of the long-
 152 term detrended data, and so additionally removed from the detrended data in order to ob-
 153 tain $x_{f_c}(t)$. Notice, that this data series, although stationary, potentially still contains some
 154 temporal correlation emerging from both spatial and temporal meteorological circulation
 155 dynamics in the atmosphere. Therefore, $x_{f_c}(t)$ was still further decomposed into a determin-
 156 istic and a stochastic fluctuation representing the intrinsic noise resulting from such complex
 157 dynamics. The time series $x_{f_c}(t)$ was then standardized, i.e. by subtracting the mean and by
 158 dividing by its standard deviation, to obtain a series $x'_{f_c}(t)$ having zero mean and unit vari-
 159 ance. As the temporal correlation affecting the standardised data had almost an exponential
 160 decreasing structure, we opted to remove it by means of linear stochastic models, e.g. like
 161 the AutoRegressive AR(p) model of p^{th} -order (Eq. 3) (Maidment et al., 1993; Salas et al.,
 162 1985; Haltiner and Salas, 1988)

$$x'_{f_c}(t) = \sum_{j=1}^p \phi_j(x'_{f_c}(t-j) - \mu) + \varepsilon_t, \quad (3)$$

163 with p autoregressive parameters $\phi(1), \dots, \phi(p)$. The noise ε_t in Eq. (3) is an uncorrelated
 164 gaussian process with zero mean and unit variance (Maidment et al., 1993). The data was
 165 checked for the most suitable AR model order by computing the sample autocorrelation
 166 (ACF) and the partial autocorrelation functions (PACF) (Brockwell and Davis, 2016), whose
 167 expressions are well known and will here be omitted. The most suitable AR model for each
 168 time series was then tested to remove any correlation in the residuals, and later used for
 169 generating statistically equivalent time series as well for forecasting purposes (Brockwell
 170 and Davis, 2016).

171 2.4 Modeling the slow component $x_s(t)$

172 The long-term trend, $x_s(t)$ affecting each data series led us hypothesize the presence of a
 173 low-dimensional dynamics linking the three variables, sunshine duration, precipitation and

174 air temperature at such time scales. This is motivated by the fact that sunshine duration gov-
 175 erns soil-atmosphere heat exchange processes, evapotranspiration among which drives pre-
 176 cipitation depending on air temperature conditions, which all feedback on sunshine duration.
 177 At large time scales, one would therefore expect that such three variables may well represent
 178 the average status of the climate of the region and can therefore be adopted as state variables
 179 of the dynamical system. In turn, this motivates the seek of a dynamical model mimicking
 180 the data that may help understanding toward which long-term dynamics the system is point-
 181 ing. We therefore adopted a dynamical systems type of approach and hypothesized that such
 182 a (climate) system is currently being evolving along a non-stationary trajectory as a result
 183 of the 3-dimensional autonomous system of Ordinary Differential Equation (ODEs)

$$\begin{cases} \dot{x} = f_s(x, y, z) \\ \dot{y} = f_p(x, y, z) \\ \dot{z} = f_T(x, y, z) \end{cases}, \quad (4)$$

184 where $x(t)$, $y(t)$ and $z(t)$ are sunshine duration, precipitation, and air temperature, re-
 185 spectively and t is time. In particular, the three scalar functions were chosen in the form of a
 186 simple complete 3-order polynomial

$$\begin{cases} \dot{x} = c_{1,1} + c_{1,2}x + c_{1,3}y + c_{1,4}z + \dots + c_{1,20}z^3 \\ \dot{y} = c_{2,1} + c_{2,2}x + c_{2,3}y + c_{2,4}z + \dots + c_{2,20}z^3 \\ \dot{z} = c_{3,1} + c_{3,2}x + c_{3,3}y + c_{3,4}z + \dots + c_{3,20}z^3 \end{cases}, \quad (5)$$

187 where $c_{i,k}$ are the coefficients to be optimized. For the optimization process of such a
 188 strongly nonlinear system we appealed to a system identification techniques working in the
 189 phase space and named "Trajectory Method" (Eisenhammer et al., 1991; Perona et al., 2000).
 190 This methodology compares the model performance against the observed system trajectory
 191 in the phase space $x(t), y(t), z(t)$ and for each component builds the quality function

$$Q^i = \sum_{j=1}^{j_{max}} \sum_{l=1}^{l_{max}} \|x_m^j(t_j + \Delta t_l) - x_r^j(t_j + \Delta t_l)\|, \quad (6)$$

192 for j_{max} initial conditions taken on the observed variable $x_r(t)$ and let the model variable
 193 $x_m(t)$ to evolve for a time $t_l = \Delta t 2^{l-1}$, ($l, 1..l_{max}$) (e.g., see Perona et al. (2000) for details).
 194 Optimum values of the coefficients $c_{i,k}$ are then obtained through a minimization process of
 195 quality function (Eq. 6) using the least-squares method (Eisenhammer et al., 1991; Perona
 196 et al., 2000). When the level of noise in the observed data is not too high, then the model
 197 would converge ideally by switching off those coefficients corresponding to the monomial
 198 terms that do not contribute to the dynamics (Perona et al., 2000). This methodology is
 199 very robust against model instabilities and has successfully been applied to model several
 200 processes in nature (Perona et al., 1998, 2001; Perona and Burlando, 2008). We study the
 201 model dynamics from a more analytical point of view by restricting our analysis to the
 202 equilibrium points and their linear stability. By definition, equilibrium points correspond
 203 to the points in the state space where temporal derivatives of the flow nullify. Therefore,
 204 equilibrium points can be found by solving the algebraic system

$$\begin{cases} f_s(x, y, z) = 0 \\ f_p(x, y, z) = 0 \\ f_T(x, y, z) = 0. \end{cases} \quad (7)$$

From a geometrical point of view, such points are found at the intersection of the curves where each flow component has null time derivative (isoclines). In order to inquire the stability of equilibrium points we performed a linear stability analysis, whose details can be found in any analytical mechanics books, e.g. see (Strogatz, 2018) Here it suffices to recall that the main steps of the linear stability analysis are to first linearize the model (Eq. 5) and then to calculate the corresponding eigenvalues of the matrix of the first order partial derivatives (Jacobian matrix) at each equilibrium point. The sign (i.e., positive or negative) and the domain (i.e., real or imaginary) of the eigenvalues define the stability properties of the equilibrium point along the principal axes of the phase space.

2.5 Universal Thermal Climate Index - UTCI

UTCI is the common index used to assess bioclimatic conditions because of its general applicability across the year (Havenith et al., 2012). The variability of UTCI describes hot and cold human comfort responses on outdoor environment. Because of its definition, the UTCI is the most comprehensive index involving parameters such as air temperature (T), wind speed (v), water vapour pressure (e) and mean radiant temperature (T_{mrt}) (Fiala et al., 2012),

$$UTCI = f(T, v, e, T_{mrt}). \quad (8)$$

Water vapour pressure and mean radiant temperature can be calculated from sunshine duration, precipitation and mean air temperature, whereas wind speed is generically assumed constant and used as a sensitivity parameter. In particular, mean radiant temperature, T_{mrt} , was calculated from sunshine duration by using the SolAlt formula from MENEX 2005 (Błażejczyk, 2005) and implemented in the Bioklima software (Błażejczyk, 1996):

$$T_{mrt} = \left(\frac{R}{Irc} + 0.5L_g + 0.5L_a \right)^{0.25} - 273. \quad (9)$$

In eq. (9), R is absorbed solar radiation ($W \cdot m^{-2}$), Irc is the coefficient reducing convective and radiative heat transfer through clothing, L_g is ground radiation ($W \cdot m^{-2}$), L_a is atmosphere back radiation ($W \cdot m^{-2}$), s_h - emissivity coefficient for humans (0.95) and σ is the Stefan-Boltzmann constant ($5.667 \cdot 10^{-8} W \cdot m^{-2} \cdot K^{-4}$). Absorbed solar radiation (R) was calculated using the SolAlt model based on cloudiness (N [%]) and position of the Sun (hSI [°]) and detailed formulas are published Błażejczyk (2005). For monthly data the position of the Sun was taken from the middle position in each month. The water vapour pressure for the data was reconstructed and homogenized following Bryś and Bryś (2010b) and modelled using Tetens' formula (Tetens, 1930).

Eventually, mean monthly values of the independent variables defining the UTCI, were all inside the range of the limiting conditions of applicability so that the UTCI could easily be computed using the Bioklima software (Havenith et al., 2012).

Our data analysis and modelling of sunshine duration, precipitation and temperature was then useful to obtain projections of such variables at long-term, and then the UTCI of the region. In particular, this was done by generating synthetic data from re-aggregation of the slow and the fast components, i.e. as per Eq.(2).

In order to analyze the sensitivity of the UTCI model to wind speed conditions, we used 0.5, 1, and 5 m/s. For this wind speed scenarios we both reconstructed UTCI values for the 117 years of available data and performed long-term calculations in order to explore UTCI variability at long term.

246 3 Results

247 3.1 Signal decomposition: the slow and the fast components

248 Figure 2 shows the long-term trends (red curves) that emerged for each time series as a result
 249 of the moving average and the Butterworth low-pass filter with a cutting frequency of 0.0038
 250 Month^{-1} . After removing the small artificial delay introduced by the moving average and the
 251 filter, the trend was adopted as slow component and removed from the original data in order
 252 to make them stationary. Whilst the trend behaviour for sunshine duration and precipitation
 253 appear fluctuating almost with zero mean, the one for temperature clearly shows a positive
 254 drift affecting the last years of the series in agreement with climate observations of ongoing
 255 changes. The relatively clear behaviour of the three series leaves also to suppose the presence
 256 of a low-dimensional dynamics underneath the data and linking such three climatic variables
 257 in a deterministic fashion. This aspect will be further addressed in section 3.2 ahead.

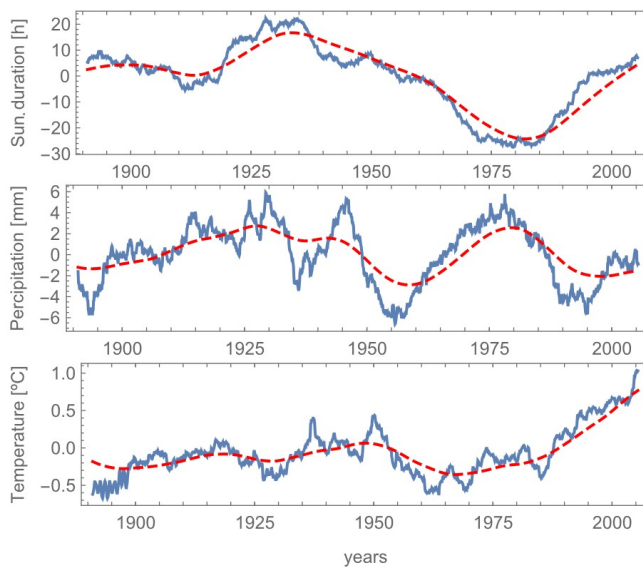


Fig. 2 Ten years moving average (blue line) and non-linear trend (dashed red line) obtained from filtering the moving averaged data with a Butterworth low-pass filter.

258 After removing the trend, the resulting time series $x_f(t)$ was de-seasonalized and then
 259 standardized to obtain $x'_f(t)$ (Figure 3, mid panels). Both sunshine duration and precipitation
 260 show the presence of a weak but statistically significant temporal autocorrelation, which
 261 indicates that fluctuations in the series do not have a completely random (i.e., white noise)
 262 origin, but still present a deterministic dependency on previous data back to some time lag
 263 and only statistically non-significant residual oscillations (Fig 3 top panels). In particular,
 264 sunshine duration shows a significant correlation with previous data up to lag 1, precipitation
 265 up to lag 2 and temperature none.

266 The Autoregressive models (Eq. 3) described in Section 2 were then used (AR(1) for
 267 sunshine duration and AR(2) for precipitation) to remove the residual correlation, thus leav-
 268 ing completely uncorrelated residuals (Figure 3 lower panels). We concluded that the fast

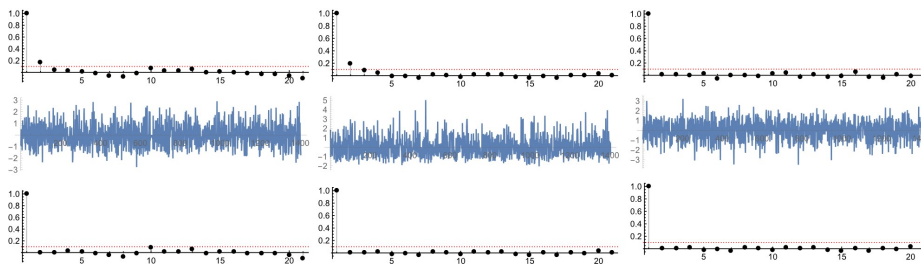


Fig. 3 Autocorrelation function (ACF) of sunshine duration, precipitation and air temperature(upper) with residuals of Autoregressive models (AR) (middle) and test of autocorrelation by ACF of residual (bottom) for each meteorological parameter

269 component of such climatic time series is composed of deterministic seasonal fluctuations,
 270 plus colored noise that can easily be replicated or synthesized by means of simple linear
 271 autoregressive models.

272 **3.2 The slow-component as dynamical system**

273 The three time series forming the slow component were analyzed with the Trajectory Method
 274 (sec. 2.4) in order to seek for a low-dimensional dynamical system explaining the mechanistic
 275 structure underlying the data. When using a number of initial states , $j_{max} = 48$, with an
 276 inter-distance between them $d = 7$ and sequential model evolutions up to 25 data ($l_{max} = 4$)
 277 per each initial condition, the Trajectory Method returned a set of coefficients describing a
 stable 3D dynamical system that mimicked both the single time series and their trajectory

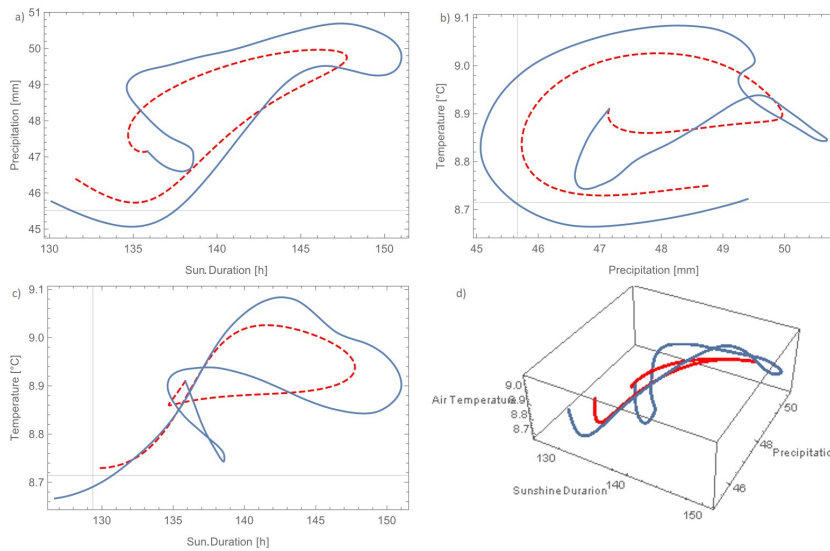


Fig. 4 Phase space data compared to model results of precipitation and sunshine duration (a), air temperature precipitation (b), temperature and sunshine duration (c) and 3-dimensional phase space (d)

278 in the phase space (Fig 4). It has to be stressed that the reconstruction technique was un-
 279 successful in the majority of the trials run by changing reconstruction parameters (3600 total
 280 trials). Only in about 17 cases the method returned a stable system and only in about 5 cases
 281 the system reproduced to some similarity the system trajectory, in some cases diverging on
 282 the long term. The parameter set presented here was the only one that represented a sta-
 283 ble dynamical system with the minimum error function. The scarcity of meaningful models
 284 found by the method is surprising given the elevated number of coefficient involved. Despite
 285 having low physical meaning, polynomial models with such a high number of coefficients
 286 usually guarantee a high flexibility in reproducing the observed data (Perona et al., 2000).
 287 To some extent this evidences the uniqueness of the model that is able to reproduce such
 288 a complex dynamic behaviour, as shown in Figure 4. Panels a)-d) show the projection of
 289 the phase space along all 2-D variable pairs as well as the 3-D phase space trajectory. The
 290 measured data are qualitatively well represented, although quantitatively some differences
 291 are clearly evident. The cumulative density functions (Fig. 5 middle) shows a very good
 292 estimation of precipitation but an overestimation of the air temperature values in the range
 293 between 8.9 and 9.1 °C (Fig. 5 right). Sunshine duration is instead underestimated in the
 294 range between 110 and 135 $\frac{h}{month}$ (Fig. 5 left).

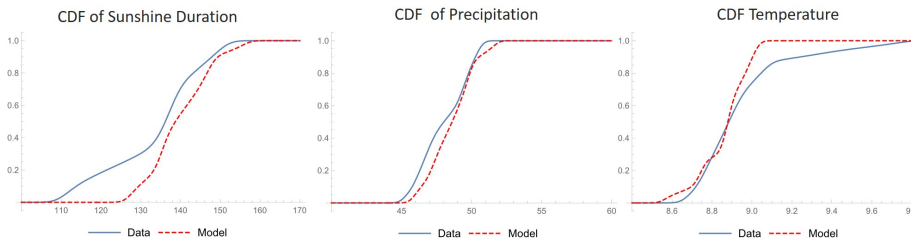


Fig. 5 Cumulative density function (CDF) for the measured and modeled time-series of sunshine duration, precipitation and air temperature in Wrocław

295 The underestimated values of the hours of sunshine duration are strongly related with
 296 the overestimated values of air temperature in last twenty years. This relationship has thus
 297 low physical sense, because air temperature would rise despite the less energy income from
 298 the Sun. Mutual strong relationship between all measured variables in the model will be
 299 further explained in the next section.

300 Despite the lack of information of pollutant, ozone's and other parameters that are con-
 301 sidered direct responsible of global warming (Stocker et al., 2013), the model shows a very
 302 similar behavior to the analyzed time-series in Wrocław for the last twenty years. It is there-
 303 fore instructive to study its dynamical properties in order to inquire the system behavior at
 304 long-term.

305 3.3 Slow component dynamical properties: long-term attractor, equilibrium points and 306 related stability

307 The model of the slow component represents the dynamic behaviour of an autonomous,
 308 nonlinear and strongly dissipative system. Assuming that the real system is currently expe-
 309 riencing a transient dynamics undergoing climate changes, the model might provide some

310 insights about the asymptotic behaviour of the real system under present environmental
311 constraints. In other words, the model evolution at long-term will occur towards an attrac-
312 tor, that is the geometrical object in the phase space representing the topological manifold
313 of the dynamics.

314 From a purely numerical point of view, the model shows to converge onto a periodic
315 behavior for all variables as shown from the projection of the phase space (Fig. 6a-c). In
316 the phase space, this results into a 3D closed trajectory that attracts the ODEs' system when
317 started from any initial conditions taken within the 'so-called' basin of attraction (Fig. 6d).
318 To this regard, Figs. 6 show the outcome of the model after 7000 iterations, which cor-
319 respond to about 583 years (117 reconstructed and 466 forecast). The length of available
320 observations clearly belong to the initial transient phase of the model, which appears then
321 to stabilize onto a periodic pattern after some periods (Fig. 6e). The periodicity of the oscil-
322 lations is about 642 months (i.e., 53.5 years). This oscillation may be related to the Atlantic
323 Multidecadal Oscillation (AMO), which has an approximate periodicity ranging between
324 55-80 years (see also the Discussion section ahead). The stability analysis of the model
325 shows that the model has only four real equilibrium points (Sec. 2.4 Eq. 7), which are, for
326 the sake of our discussion, the interesting ones (Tab. 1). Equilibrium points are shown in
327 the phase space (Fig. 6d). Equilibrium points can be either stable or unstable in the sense
328 that they either attract or repel model trajectories in the phase space, respectively. Tab. 1
329 shows that all equilibrium points have no eigenvalues with zero real part. Mathematically,
330 this ensures that all equilibrium points are 'hyperbolic', that is the stability properties of the
331 linear system are representative of those of the nonlinear one in the vicinity of the equilib-
332 rium points. Moreover, all equilibrium points have at least one eigenvalue with real positive
333 part, which means that all equilibrium points are unstable at least along one direction.

334 In our model P_1 and P_4 behave as unstable focus in the (X,Y) plane, and as stable nodes
335 along the Z direction. Thus, trajectories spiral away from the equilibrium point in the X,Y
336 plane, whereas are straightly attracted towards the point along Z. Equilibrium point P_2 is
337 instead unstable in all directions. Next to point P_3 trajectories will spiral toward the point in
338 the X,Y plane and be straightly repelled along Z. Overall, we can therefore conclude that the
339 system is locally unstable in the vicinity of the equilibrium points where trajectory would
340 sooner or later drift away from the points. However, as we verified numerically, the system
341 is globally stable because of the presence of the limit cycle, which is an actual invariant
342 manifold of the system and result from the interplay between attraction and repulsion of
343 the equilibrium point along the three coordinate axes X,Y,Z. The stability properties of the
344 limit cycle could be well investigated by mean of Floquet theory (Strogatz, 2018), which
345 is however not object of the present work. The significance and implications for the slow
346 component of the system dynamical properties presented above will be discussed in the next
347 section.

348 3.4 Reconstruction and prediction of bioclimatic conditions of the outdoor environment

349 Assessment of outdoor environment for both the actual and modeled case was made by
350 means of the UTCI, which was calculated as explained in Section 2. UTCI was calculated
351 from non-linear slow component obtained from the data or from the modeled slow compo-
352 nent. Values of UTCI monthly data oscillate in a range from -15 to 30 °C and both UTCI
353 (i.e., from data or from modelled data) agree very well in average, which reaches about 15.2
354 °C UTCI (Fig. 7 upper left). Changes of UTCI calculated from slow components are in the
355 range between 10.5 and 15 °C UTCI. The mean square error (MSE) between modeled and

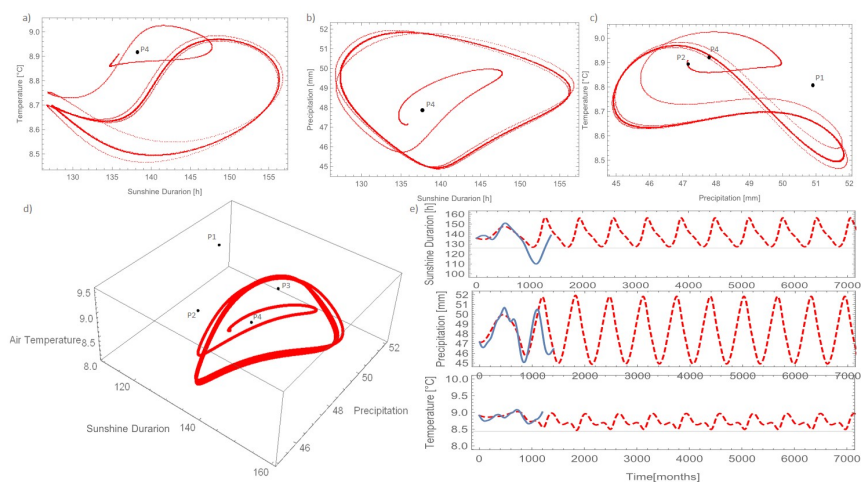


Fig. 6 Long term prediction for model in phase space's of sunshine duration, precipitation and air temperature (a-c), 3-d dimensional space with equilibrium points (d) and long term courses of analyze all components with original trend (e).

Table 1 Equilibrium points and related eigenvalues defining their characteristics

Points	Equilibrium points	Eigenvalues
Sunshine Duration [X_1]	110.481	$0.0164 + 0.0133i$
Precipitation [Y_1]	51.145	$0.0164 - 0.0133i$
Temperature [Z_1]	8.798	-0.0163
Sunshine Duration [X_2]	125.214	$0.00044 + 0.0133i$
Precipitation [Y_2]	47.316	$0.00044 - 0.0133i$
Temperature [Z_2]	8.890	0.0069
Sunshine Duration [X_3]	130.006	$-0.0115 + 0.0206i$
Precipitation [Y_3]	51.314	$-0.0115 - 0.0206i$
Temperature [Z_3]	8.378	0.0224
Sunshine Duration [X_4]	138.049	$0.001821 + 0.00776i$
Precipitation [Y_4]	47.908	$0.00182 - 0.00776i$
Temperature [Z_4]	8.923	-0.00541
Points	Characteristic	
$P_1(X_1, Y_1, Z_1)$	unstable focus in (X,Y), stable node along Z	
$P_2(X_2, Y_2, Z_2)$	unstable focus in (X,Y), unstable node along Z	
$P_3(X_3, Y_3, Z_3)$	stable focus in (X,Y), unstable node along Z	
$P_4(X_4, Y_4, Z_4)$	unstable focus in (X,Y), stable node along Z	

356 obtained slow component from data is equal 0.076 what was also identified on a comparison
 357 of those time series at probability density function (Fig. 7, upper right). Comparison of 1
 358 m/s and 5m/s approaches was presented on the bottom panels of Figure 7. By increasing the
 359 wind speed the difference in compatibility between reconstructed and real data increases.
 360 MSE on 5 m/s scenario increase to 0.15. The differences between the subtracted and mod-

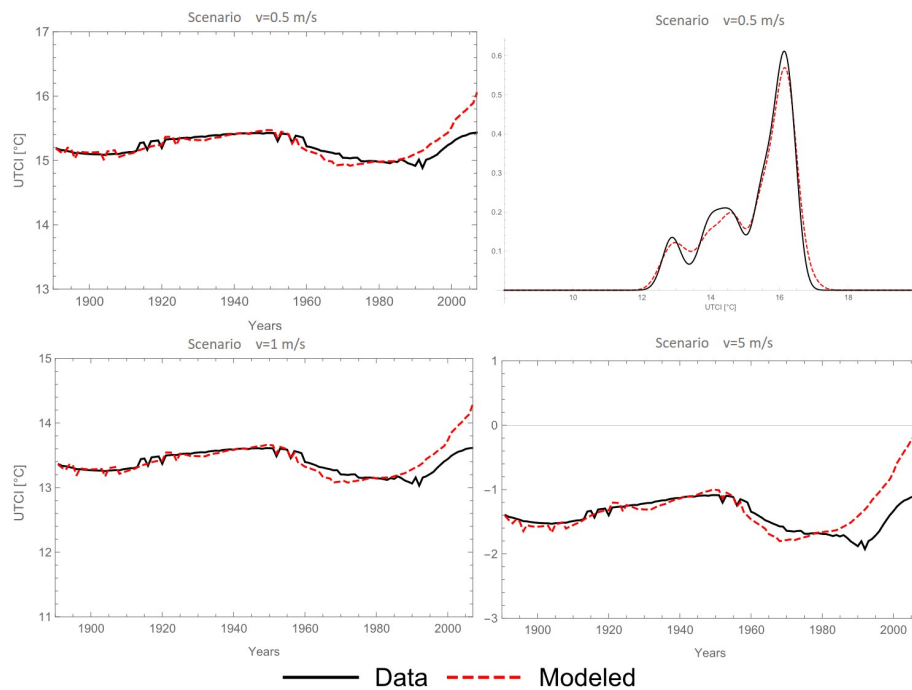


Fig. 7 Monthly UTCI values for 0.5 m/s scenario with comparison of probability density functions (upper panels) with UTCI in two other scenarios (1, 5 m/s) for data and modeled slow component time series.

361 eled slow component in assessment of the UTCI significantly change. The most impacted
 362 element in shaping UTCI values is air temperature. The worst predicted temperature, with
 363 maximum error about 0.2 °C (Fig. 6), caused big changes in sunshine duration and precipi-
 364 tation mostly because scale of units. This change is less relevant in the bioclimatic outdoor
 365 environmental assessment than in global climate changes, where air temperature is also the
 366 most responsive parameter. This small variance of air temperature in the model may have
 367 application in reconstructing and forecasting the bioclimatic outdoor environmental condi-
 368 tions. Despite the annual average the long term oscillation is still visible. In the analyzed
 369 period 1891-2007 one sees that two minimum values occur in a range of 60-80 years. In
 370 order to better enhance the periodicity only one wind scenario was used for the forecast of
 371 the UTCI (0.5 m/s).

372 Figure 8 shows the comparison of the UTCI computed from the modelled slow com-
 373 ponent and the observed one for lowest wind-speed scenario. Both UTCI show similar be-
 374 haviour and the modeled one allow for a long-term forecast of the underlying trend. Ac-
 375 cording to the dynamics of the slow component an oscillating trend will establish under
 376 the assumption that present boundary (atmospheric and environmental) conditions do not
 377 change.

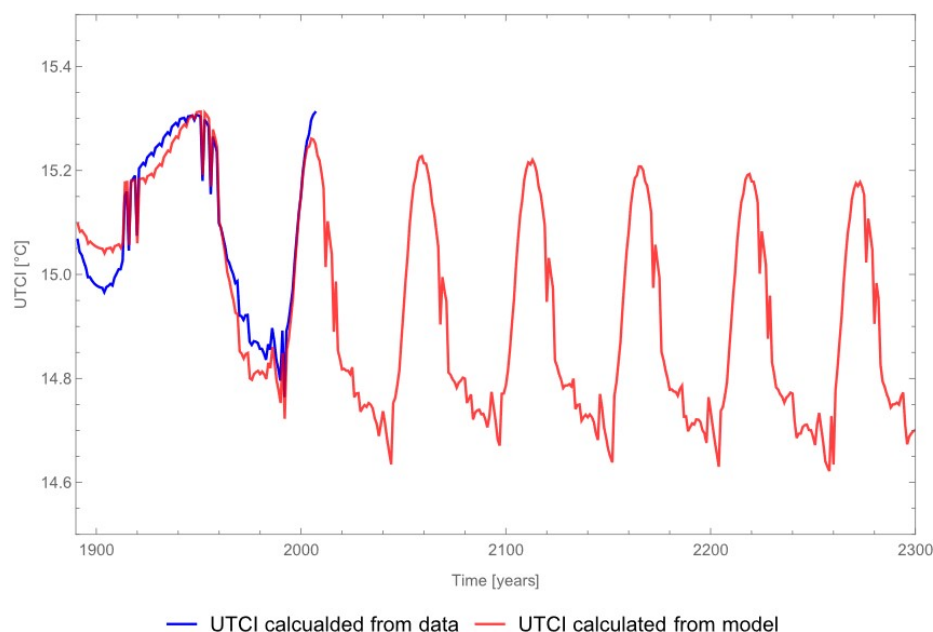


Fig. 8 Long term prediction of decadal variability of UTCI trend compared to data obtained from slow component time series for the 0.5 m/s wind speed scenario.

378 4 Discussion

379 Stochastic and deterministic approaches have been used to model environmental processes
 380 (Perona and Burlando, 2008; Chalfen et al., 2014; Czernecki et al., 2018; Malik et al., 2018),
 381 financing (Campbell et al., 1997), city transport (Kazak et al., 2017), quality assessment (De-
 382 Lone and McLean, 1992) and many others processes. Time series analysis of measured data
 383 may reveal the presence of low-dimensional deterministic behaviour in the slow component
 384 (e.g., the long-term trend). The corresponding dynamical system can sometimes be recon-
 385 structed starting from observations (Baake et al., 1992; Eisenhammer et al., 1991; Judd and
 386 Mees, 1995; Irving and Dewson, 1997; Perona et al., 2000, 2001). Most of such techniques
 387 are today included in machine learning approaches (Czernecki et al., 2018; Pilguy et al.,
 388 2019; Szymanowski et al., 2019).

389 The effort performed here to separate all components and reconstruct their physical
 390 nature has shown that the fast component has the properties of a coloured noise possibly
 391 overlapped to a seasonal behaviour. The slow component may often hinder a dynamics with
 392 a more deterministic structure. Indeed, the three variables analysed here are representative
 393 of the average state of the climatic system, and can therefore be treated as actual state vari-
 394 ables responsible for the slow component. In other words, the state variables could be linked
 395 in a mechanistic fashion. In this study, the slow component shows a long term oscillation
 396 that made appealing the use of reconstruction techniques. Notably, the periodic oscillation
 397 that characterizes the dynamic of the reconstructed slow component would be consistent
 398 with well known patterns induced by the Atlantic Multidecadal Oscillation (AMO) of 55-
 399 80 years (Knudsen et al., 2011; Brönnimann, 2015; Malik et al., 2018). Also, Malik et al.
 400 (2018) found statistical evidence that Atlantic Multidecadal Oscillation (AMO) has intrin-

401 sic positive correlation with solar activity. Thus, after a transitory time that started in the
402 anthropocene, the model of the slow dynamics suggests that the system will set on to a pe-
403 riodic oscillation yet driven by AMO, but characterized by an offset average with respect
404 to pre-anthropoc conditions. The effect of anthropic actions are indeed implicitly appearing
405 in the behaviour of the observed variables, which is why we adopt a dynamical system ap-
406 proach that objectively aims at reconstructing the dynamics. Our model for the long-term
407 trend component describes an autonomous dynamical system (i.e., a surrogate climatic sys-
408 tem) out of equilibrium that shows a transient behaviour leading it to future periodic oscil-
409 lations different from the past ones. Hence, the model does not show who is responsible for
410 causing such a new trajectory, only it models that there is one and that this will lead to a new
411 periodic equilibrium.

412 The variability of the UTCI describing outdoor environment shows a systematic change
413 in the duration of the oscillation over the period where observations are available. Similarly,
414 difference from minimum and maximum values drastically increased as well as the time
415 of these extreme periods (Fig. 8). Colder periods with average UTCI temperature lower
416 than 15°C lasted for about 40 years and after which UTCI values drastically grew at the
417 beginnings of 80s. This is an effect of increased air temperature and sunshine duration which
418 resulted in less frequent cloud cover (sec. 3.3). Decreasing of UTCI in present years is
419 mainly caused by less frequent precipitation periods that determine air water content. In
420 terms of bioclimatic outdoor environment, the Wroclaw case (central Europe climate) shows
421 increasing air temperature and hours of sunshine duration, decrease a heat sensations of
422 human body because of less humidity in the air. This situation might of course be different
423 in other parts of the world where air humidity is already low, and air temperature is at
424 different level then in Wroclaw (central Europe).

425 At longer term, the model suggests that the oscillating trend will set to a constant period-
426 icity, and generically lower mean. This is an effect of air temperature and sunshine duration
427 form the model. According to figure 6 reconstructed air temperature change in bigger oscil-
428 lation (having also lower values about 0.1°C) than data. Reconstructed precipitation data
429 oscillate in bigger range then raw data. In the other hand sunshine duration is overestimated.
430 These small differences indicate those changes in UTCI. This was also visible in Głogowski
431 et al. (2020) about the bioclimatic conditions of the Lower Silesia where UTCI was almost
432 constant despite increasing air temperature. Bioclimatic conditions are "sum" of all outdoor
433 environmental conditions. The changes in air temperature may be overtaken by other factors
434 like humidity, solar radiation or wind speed. In this case, the model overestimates sunshine
435 duration and underestimates air temperature. The amount of precipitation was reconstructed
436 with the best correspondence to raw data.

437 As stated in the introduction, UTCI found broad application to describe outdoor envi-
438 ronmental conditions in many parts of the world, and may help sustaining the economic
439 growth of low-income countries Sen and Nag (2019). The technique developed in this work
440 may be useful either for reconstructing past and future UTCI dynamics or to simply generate
441 synthetic data for filling data gaps or for statistical analyses. Another potential application
442 could be downscaling data to regions that do not possess meteorological observations.

443 Perhaps in a speculative way, we attempt an interpretation of our model results keep-
444 ing in mind that our model is only indirectly physically based because it entirely builds on
445 the (nonlinear) information contained in observed data. As such the autonomous dynamical
446 system that was reconstructed for the slow component does not include the effect of further
447 forcing on the state variables. Under these premises, the data trend dynamics would sug-
448 gest that present conditions would actually sit on a transient climatic trajectory, which will
449 lead outdoor environmental conditions for the region to settle on a periodic long term be-

450 haviour for the trend. The persistent increase of sunshine duration and temperature averages
451 will eventually feedback on precipitation. Future years may then experience a precipitation
452 increase and consequent decrease of sunshine duration and temperature with some phase
453 delay (already present in the observations) probably due to thermal inertia of air and water
454 masses. Hence, current transient conditions clearly emerging from observations were likely
455 triggered by past stress on the global climate caused by severe anthropic activities. This
456 seems however to not have altered the future footprint of multidecadal oscillations (e.g.,
457 AMO in particular) on the proxy climatic variables investigated here.

458 5 Conclusions

459 A non-linear approach (trajectory method) for reconstructing ordinary differential equations
460 from data was used in this paper in order to model the slow component affecting monthly
461 sunshine duration, precipitation and temperature data. The reconstructed dynamical system
462 was then used to build the aggregated UTCI representing bioclimatic conditions of the out-
463 door environment for the region of interest. Past and present evolution of UTCI seems to
464 settle on long term 50-60 years fluctuations where an as small as 0.1 °C change of monthly
465 air temperature may induce changes of monthly sum of precipitation of about 5 mm, in
466 turn causing 20 hours monthly difference in sunshine duration. Globally, this behaviour was
467 investigated in terms of UTCI, which is however strongly dependent on wind speed as a pa-
468 rameter. The mean square error for low wind speed (0.5 m/s monthly value) values was very
469 low and equal to 0.07 and for high wind speed (5 m/s monthly value) increase to 0.15. Our
470 modelling approach is general and can be applied to any environment provided that long
471 enough time series of measured data are available.

472
473 **Acknowledgements** A.G would like to acknowledge the School of Engineering and the Institute for In-
474 frastructure and Environment of the University of Edinburgh for hosting him during his three visits to the
475 Chair of Environmental Engineering in 2019 and 2020. P.P. would like to thank Stefan Brönnimann for useful
476 discussion about AMO.

477 References

- 478 Baake E, Baake M, Bock H, Briggs K (1992) Fitting ordinary differential equations to
479 chaotic data. *Physical Review A* 45(8):5524, DOI 10.1103/PhysRevA.45.5524
- 480 Błażejczyk K (1996) *BioKlima 2.6*. Institute of Geography and Spatial Organization
481 (<http://www.igipz.pan.pl/Bioklima-zgik.html>), [Online; accessed 19-01-2019]
- 482 Błażejczyk K (2005) *Menex2005* the updated version of man-environment heat exchange
483 model. URL [https://www.igipz.pan.pl/tl_files/igipz/ZGiK/opracowania/
484 indywidualne/blazejczyk/MENEX_2005.pdf](https://www.igipz.pan.pl/tl_files/igipz/ZGiK/opracowania/indywidualne/blazejczyk/MENEX_2005.pdf), [Online; accessed 19-01-2019]
- 485 Błażejczyk K, Kunert A (2011) *Bioclimatic principles of recreation and tourism in Poland*
486 (in Polish), vol 13
- 487 Błażejczyk K, Bröde P, Fiala D, Havenith G, Holmér I, Jendritzky G, Kampmann B, Kunert
488 A (2010) Principles of the new Universal Thermal Climate Index (UTCI) and its appli-
489 cation to bioclimatic research in European scale. *Miscellanea Geographica* 14(2010):91-
490 102, DOI 10.2478/mgrsd-2010-0009

- 491 Błażejczyk K, Epstein Y, Jendritzky G, Staiger H, Tinz B (2012) Comparison of UTCI to
492 selected thermal indices. *International Journal of Biometeorology* 56(3):515–535, DOI
493 10.1007/s00484-011-0453-2
- 494 Błażejczyk K, Jendritzky G, Bröde P, Fiala D, Havenith G, Epstein Y, Psikuta A, Kampmann
495 B (2013) An introduction to the universal thermal climate index (UTCI). *Geographia*
496 *Polonica* 86(1):5–10, DOI 10.7163/GPol.2013.1
- 497 Bosford JH (1971) A wet globe thermometer for environmental heat measure-
498 ment. *American Industrial Hygiene Association Journal* 32(1):1–10, DOI 10.1080/
499 0002889718506400, URL <https://doi.org/10.1080/0002889718506400>, PMID:
500 5540211, <https://doi.org/10.1080/0002889718506400>
- 501 Brockwell PJ, Davis RA (2016) *Introduction to time series and forecasting*. Springer
- 502 Bröde P, Krüger EL, Rossi FA, Fiala D (2012) Predicting urban outdoor thermal comfort
503 by the Universal Thermal Climate Index UTCI—a case study in Southern Brazil. *Inter-
504 national Journal of Biometeorology* 56(3):471–480
- 505 Bröde P, Fiala D, Lemke B, Kjellstrom T (2018) Estimated work ability in warm outdoor
506 environments depends on the chosen heat stress assessment metric. *International Journal*
507 *of Biometeorology* 62(3):331–345, DOI 10.1007/s00484-017-1346-9
- 508 Brönnimann S (2015) Climatic changes since 1700. In: *Climatic Changes Since 1700*,
509 Springer, pp 167–321
- 510 Bryś K, Bryś T (2001) Evaporation in wrocław and its variability in the years 1946–1995.
511 *Geographia Polonica* 74:1
- 512 Bryś K, Bryś T (2003) Fluctuations of global solar radiation in 20th century at Wrocław
513 and their relations to Wolf’s number and circulation changes. *Acta Univ Wratisl St Geogr*
514 2542:189–202
- 515 Bryś K, Bryś T (2005) Zmienność warunków higrycznych we wrocławiu-swojcu w latach
516 1883–2003 (in polish). *Acta Agrophysica* 5(3):543–554
- 517 Bryś K, Bryś T (2010a) The first one hundred years (1791–1890) of the wrocław air tem-
518 perature series. In: *The Polish climate in the European context: an historical overview*,
519 Springer, pp 485–524, DOI 10.1007/978-90-481-3167-9_25
- 520 Bryś K, Bryś T (2010b) Reconstruction of the 217-year (1791–2007) wrocław air tempera-
521 ture and precipitation series. *Bulletin of Geography Physical Geography Series* 3(1):121–
522 171, DOI 10.2478/bgeo-2010-0007
- 523 Bryś K, Ojrzyńska H (2016) Stimulating qualities of biometeorological conditions in
524 Wrocław(in Polish). *Acta Geographica Lodziensia* 104:193–200
- 525 Bryś K, Bryś T, Ojrzyńska H, Sayegh MA, Głogowski A (2020) Variability and role of long-
526 wave radiation fluxes in the formation of net radiation and thermal features of grassy and
527 bare soil active surfaces in wrocław. *Science of The Total Environment* p 141192
- 528 Bryson RA (1974) A perspective on climatic change. *Science* 184(4138):753–760
- 529 Brönnimann S, Allan R, Ashcroft L, Baer S, Barriendos M, Brázdil R, Brugnara Y, Brunet
530 M, Brunetti M, Chimani B, Cornes R, Domínguez-Castro F, Filipiak J, Founda D, Herrera
531 RG, Gergis J, Grab S, Hannak L, Huhtamaa H, Jacobsen KS, Jones P, Jourdain S, Kiss
532 A, Lin KE, Lorrey A, Lundstad E, Luterbacher J, Mauelshagen F, Maugeri M, Maughan
533 N, Moberg A, Neukom R, Nicholson S, Noone S, Nordli Ólafsdóttir KB, Pearce PR,
534 Pfister L, Pribyl K, Przybylak R, Pudmenzky C, Rasol D, Reichenbach D, Řezníčková
535 L, Rodrigo FS, Rohr C, Skrynyk O, Slonosky V, Thorne P, Valente MA, Vaquero JM,
536 Westcott NE, Williamson F, Wyszynski P (2019) Unlocking pre-1850 instrumental mete-
537 orological records: A global inventory. *Bulletin of the American Meteorological Society*
538 100(12):ES389–ES413, DOI 10.1175/BAMS-D-19-0040.1, URL [https://doi.org/
539 10.1175/BAMS-D-19-0040.1](https://doi.org/10.1175/BAMS-D-19-0040.1), <https://doi.org/10.1175/BAMS-D-19-0040.1>

- 540 Campbell JY, Champbell JJ, Campbell JW, Lo AW, Lo AW, MacKinlay AC (1997) The
541 econometrics of financial markets. Princeton University Press
- 542 Chabior M (2011) Selected aspects of the bioclimate of Szczecin (in Polish). *Prace i Studia*
543 *Geograficzne* 47:293–300
- 544 Chalfen M, Łyczko W, Pływaczyk L (2014) The prognosis of influence of the Oder River
545 waters dammed by Malczyce barrage on left bank areas. *Journal of Water and Land De-*
546 *velopment* 21(1):19–27, DOI 10.2478/jwld-2014-0010
- 547 Coutts AM, White EC, Tapper NJ, Beringer J, Livesley SJ (2016) Temperature and human
548 thermal comfort effects of street trees across three contrasting street canyon environments.
549 *Theoretical and Applied Climatology* 124(1-2):55–68, DOI 10.1007/s00704-016-1832-8.
- 550 Czernecki B, Nowosad J, Jabłońska K (2018) Machine learning modeling of plant phenol-
551 ogy based on coupling satellite and gridded meteorological dataset. *International Journal*
552 *of Biometeorology* 62(7):1297–1309, DOI 10.1007/s00484-018-1534-2
- 553 Czernecki B, Głogowski A, Nowosad J (2020) Climate: An r package to access free in-
554 situ meteorological and hydrological datasets for environmental assessment. *Sustainabil-*
555 *ity* 12(1), DOI 10.3390/su12010394, URL [https://www.mdpi.com/2071-1050/12/](https://www.mdpi.com/2071-1050/12/1/394)
556 [1/394](https://www.mdpi.com/2071-1050/12/1/394)
- 557 DeLone WH, McLean ER (1992) Information systems success: The quest for the dependent
558 variable. *Information systems research* 3(1):60–95
- 559 Di Napoli C, Pappenberger F, Cloke HL (2018) Assessing heat-related health risk in Europe
560 via the Universal Thermal Climate Index (UTCI). *International Journal of Biometeorol-*
561 *ogy* 62(7):1155–1165, DOI 10.1007/s00484-018-1518-2
- 562 Dubicka M (1994) Influence of atmospheric circulation on the formation of climate
563 conditions (on the example of Wrocław) (in polish). 1581, Wydawn. Uniwersytetu
564 Wrocławskiego
- 565 Eisenhammer T, Hübler A, Packard N, Kelso JS (1991) Modeling experimental time series
566 with ordinary differential equations. *Biological cybernetics* 65(2):107–112, DOI 10.1007/
567 [BF00202385](https://doi.org/10.1007/BF00202385)
- 568 Fiala D, Havenith G, Bröde P, Kampmann B, Jendritzky G (2012) UTCI-Fiala multi-node
569 model of human heat transfer and temperature regulation. *International Journal of Biome-*
570 *eteorology* 56(3):429–441, DOI 10.1007/s00484-011-0424-7
- 571 Flohn H (1957) Large-scale aspects of the “summer monsoon” in south and east asia. *Journal*
572 *of the Meteorological Society of Japan Ser II* 35:180–186
- 573 de Freitas CR, Grigorieva EA (2017) A comparison and appraisal of a comprehensive range
574 of human thermal climate indices. *International Journal of Biometeorology* 61(3):487–
575 512, DOI 10.1007/s00484-016-1228-6
- 576 Galan JC, Guedes J (2019) Applicability of heat stress index in the context of military work:
577 Pilot study. In: *Occupational and Environmental Safety and Health*, Springer, pp 313–322,
578 DOI 10.1007/978-3-030-14730-3_34
- 579 Ge Q, Kong Q, Xi J, Zheng J (2017) Application of UTCI in China from tourism
580 perspective. *Theoretical and Applied Climatology* 128(3-4):551–561, DOI 10.1007/
581 [s00704-016-1731-z](https://doi.org/10.1007/s00704-016-1731-z)
- 582 Girs A (1971) Long-term fluctuations of the atmospheric circulation and hydrometeorolog-
583 ical forecasts. *Hydrometeorological Monographs*, St Petersburg, Russia
- 584 Groveman BS, Landsberg HE (1979) Simulated northern hemisphere temperature depart-
585 ures 1579-1880. *Geophysical Research Letters* 6(10):767–769
- 586 Głogowski A, Bryś K, Perona P (2020) Bioclimatic conditions of the Lower Silesia region
587 (South West Poland) from 1966-2017. *International Journal of Biometeorology* DOI 10.
588 [1007/s00484-020-01970-5](https://doi.org/10.1007/s00484-020-01970-5)

- 589 Haldane J (1905) The influence of high air temperatures no. i. *Epidemiology & Infection*
590 5(4):494–513, DOI 10.1017/S0022172400006811
- 591 Haltiner JP, Salas JD (1988) Development and testing of a multivariate, seasonal arma (1, 1)
592 model. *Journal of Hydrology* 104(1-4):247–272
- 593 Havenith G, Fiala D, Błażejczyk K, Richards M, Bröde P, Holmér I, Rintamaki H, Benshabat
594 Y, Jendritzky G (2012) The UTCI-clothing model. *International Journal of Biometeorol-*
595 *ogy* 56(3):461–470
- 596 Irving A, Dewson T (1997) Determining mixed linear-nonlinear coupled differential equa-
597 tions from multivariate discrete time series sequences. *Physica D: Nonlinear Phenomena*
598 102(1-2):15–36, DOI 10.1016/S0167-2789(96)00248-5
- 599 Jendritzky G, de Dear R, Havenith G (2012) UTCI—Why another thermal index? *Internation-*
600 *al Journal of Biometeorology* 56(3):421–428, DOI 10.1007/s00484-011-0513-7
- 601 Judd K, Mees A (1995) On selecting models for nonlinear time series. *Physica D: Nonlinear*
602 *Phenomena* 82(4):426–444, DOI 10.1016/0167-2789(95)00050-E
- 603 Kazak J, Chalfen M, Kamińska J, Szewrański S, Świąder M (2017) Geo-dynamic decision
604 support system for urban traffic management. In: *Proceedings of GIS Ostrava*, Springer,
605 pp 195–207, DOI 10.1007/978-3-319-61297-3_14
- 606 Knudsen MF, Seidenkrantz MS, Jacobsen BH, Kuijpers A (2011) Tracking the atlantic mul-
607 tidecadal oscillation through the last 8,000 years. *Nature communications* 2(1):1–8, DOI
608 10.1038/ncomms1186
- 609 Kondratyev KY (2013) *Radiative heat exchange in the atmosphere*. Elsevier
- 610 Kosiba A (1948) *The climate of the Silesian Lands* (in polish). Państwowe Wrocławskie
611 Zakłady Graficzne. Okręg Północ
- 612 Kuchcik M, Błażejczyk K, Szmyd J, Milewski P, Błażejczyk A, Baranowski J (2013) *Po-*
613 *tencjał leczniczy klimatu Polski*(in Polish). Wydawnictwo Akademickie SEDNO Spółka
614 z oo
- 615 Maidment DR, et al. (1993) *Handbook of hydrology*, vol 9780070. McGraw-Hill New York
- 616 Malik A, Brönnimann S, Perona P (2018) Statistical link between external climate forcings
617 and modes of ocean variability. *Climate dynamics* 50(9-10):3649–3670
- 618 Marsz A, Styszyńska A, et al. (2019) Course of winter temperatures in Poland in the years
619 1720–2015(in Polish). *Prace Geograficzne* 2018(155):85–138
- 620 Masterson J, Richardson F (1979) *Humidex, a method of quantifying human discomfort due*
621 *to excessive heat and humidity*, Environment Canada. Atmospheric Environment Service,
622 Downsview, Ontario 151:1–79
- 623 Mayer H, Höppe P (1987) Thermal comfort of man in different urban environments. *Theo-*
624 *retical and Applied Climatology* 38(1):43–49, DOI 10.1007/BF00866252
- 625 Ndetto EL, Matzarakis A (2015) Urban atmospheric environment and human biometeorolo-
626 gical studies in Dar es Salaam, Tanzania. *Air Quality, Atmosphere & Health* 8(2):175–
627 191, DOI 10.1007/s11869-014-0261-z
- 628 Nidzgorska-Lencewicz J (2015) Variability of Human-Biometeorological Conditions in
629 Gdańsk. *Polish Journal of Environmental Studies* 24(1):215–226, DOI 10.15244/pjoes/
630 26116
- 631 Niedzielski T (2011) Is there any teleconnection between surface hydrology in poland and
632 el niño/southern oscillation? *Pure and Applied Geophysics* 168(5):871–886
- 633 Niedzielski T (2014) El niño/southern oscillation and selected environmental consequences.
634 In: *Advances in Geophysics*, vol 55, Elsevier, pp 77–122
- 635 Niedźwiedz T, Twardosz R, Walanus A (2009) Long-term variability of precipitation series
636 in east central europe in relation to circulation patterns. *Theoretical and Applied Clima-*
637 *tology* 98(3-4):337–350

- 638 Okoniewska M, Więclaw M (2013) Long-term variability of bioclimatic conditions in the
639 second half of the 20 century at noon hours in Poland based on Universal Thermal Climate
640 Index. *Journal of Health Sciences* 3(15):116–129
- 641 Otterå OH, Bentsen M, Drange H, Suo L (2010) External forcing as a metronome for atlantic
642 multidecadal variability. *Nature Geoscience* 3(10):688–694
- 643 Peng J, Yu Z, Gautam MR (2013) Pacific and atlantic ocean influence on the spatiotemporal
644 variability of heavy precipitation in the western united states. *Global and Planetary
645 Change* 109:38–45
- 646 Perona P, Burlando P (2008) Mechanistic interpretation of alpine glacierized environments:
647 Part 1. model formulation and related dynamical properties. *Advances in Water Resources*
648 31(7):937 – 947, DOI <https://doi.org/10.1016/j.advwatres.2008.03.008>, URL <http://www.sciencedirect.com/science/article/pii/S0309170808000523>
- 649 Perona P, Porporato A, Ridolfi L (1998) A simple experimental equation for the bursting
650 cycle. *Physics of Fluids* 10(11):3023–3026, DOI 10.1063/1.869823
- 651 Perona P, Porporato A, Ridolfi L (2000) On the trajectory method for the reconstruction of
652 differential equations from time series. *Nonlinear Dynamics* 23(1):13–33, DOI 10.1023/
653 A:1008335507636
- 654 Perona P, D’Odorico P, Porporato A, Ridolfi L (2001) Reconstructing the temporal dynamics
655 of snow cover from observations. *Geophysical research letters* 28(15):2975–2978
- 656 Pilguy N, Tazsarek M, Pajurek Ł, Kryza M (2019) High-resolution simulation of an isolated
657 tornadic supercell in poland on 20 june 2016. *Atmospheric research* 218:145–159, DOI
658 10.1016/j.atmosres.2018.11.017
- 659 Rozbicka K, Rozbicki T (2016) The Influence of biometeorological stimuli of air pressure
660 in relation to atmospheric circulation in Warsaw. *Acta Scientiarum Polonorum-Formatio
661 Circumiectus* 15(3):121–136
- 662 Rozbicka K, Rozbicki T (2018) Variability of UTCI index in South Warsaw depending on
663 atmospheric circulation. *Theoretical and Applied Climatology* 133(1-2):511–520, DOI
664 10.1007/s00704-017-2201-y
- 665 Salas JD, Tabios III GQ, Bartolini P (1985) Approaches to multivariate modeling of water
666 resources time series 1. *JAWRA Journal of the American Water Resources Association*
667 21(4):683–708
- 668 Sen J, Nag PK (2019) Human susceptibility to outdoor hot environment. *Science of the Total
669 Environment* 649:866–875, DOI 10.1016/j.scitotenv.2018.08.325
- 670 Stocker TF, Qin D, Plattner GK, Tignor M, Allen SK, Boschung J, Nauels A, Xia Y, Bex V,
671 Midgley PM, et al. (2013) Climate change 2013: The physical science basis. Contribution
672 of working group I to the fifth assessment report of the intergovernmental panel on climate
673 change 1535
- 674 Strogatz SH (2018) *Nonlinear dynamics and chaos with student solutions manual: With
675 applications to physics, biology, chemistry, and engineering*. CRC press
- 676 Szymanowski M, Wiczorek M, Namyślak M, Kryza M, Migala K (2019) Spatio-temporal
677 changes in atmospheric precipitation over south-western poland between the periods
678 1891–1930 and 1981–2010. *Theoretical and Applied Climatology* 135(1-2):505–518,
679 DOI 10.1007/s00704-018-2376-x
- 680 Tetens O (1930) Über einige meteorologische begriffe. *Z geophys* 6:297–309
- 681 Thilenius R, Dorno C (1925) Das Davoser Frigorimeter:(ein Instrument zur Dauerreg-
682 istrierung der physiologischen Abkühlungsgrösse). Vieweg
- 683 WMO (2009) WMO Holds Symposium on Universal Thermal
684 Climate Index. URL [http://sdg.iisd.org/news/
685 wmo-holds-symposium-on-universal-thermal-climate-index/](http://sdg.iisd.org/news/wmo-holds-symposium-on-universal-thermal-climate-index/), [Online;
686

687 accessed 19-01-2019]

688 Wu F, Yang X, Shen Z (2019) Regional and seasonal variations of outdoor ther-
689 mal comfort in China from 1966 to 2016. Science of The Total Environment
690 665:1003 – 1016, DOI <https://doi.org/10.1016/j.scitotenv.2019.02.190>, URL [http://](http://www.sciencedirect.com/science/article/pii/S0048969719306783)
691 www.sciencedirect.com/science/article/pii/S0048969719306783